569

INTRA-ANNUAL CHARACTERISTICS OF THE RELATIONSHIP BETWEEN THE SURFACE TEMPERATURE-BASED URBAN HEAT ISLAND INTENSITY AND THE LOCAL CLIMATE ZONES

Rita Pongrácz*[1,2], Judit Bartholy[1,2], Csenge Dian[1], Zsuzsanna Dezső[1]
[1]Dept. of Meteorology, Eötvös Loránd University, Budapest, Hungary
[2]Faculty of Science, Excellence Center, Eötvös Loránd University, Martonvásár, Hungary

1. INTRODUCTION

The population of the world is increasing. The artificial surface modifies the urban climate. One of the main environmental effects of the urban climate is the urban heat island (UHI). The UHI intensity is the difference between the urban and rural temperature (Oke, 1973). To determine the UHI intensity either air temperature and surface temperature can be used. The traditional UHI intensity is based on in-situ air temperature measurements (e.g. Klysik and Fortuniak, 1999; Unger et al., 2000; Pongrácz et al., 2016). To calculate the surface temperature based UHI (SUHI) radiation measurements of satellites can be used (e.g., Price, 1979; Dezső et al., 2005). The Department of Meteorology, Eötvös Loránd University, Budapest, Hungary has investigated urban climate for decades, especially the UHI and SUHI phenomenon (Pongrácz et al., 2010; Bartholy et al., 2016). To analyze the SUHI intensity the radiation and temperature data of NASA satellites were used.

The structure of the city is a determining factor in the urban climate research. Stewart and Oke (2012) defined the Local Climate Zones (LCZs) system. The built-up density and the vegetation-cover areas affect the development of SUHI intensity. LCZ classes were used for the analyses of several European (e.g. Brousse et al., 2016) and Asian cities (e.g. Cai et el., 2016).

In this paper, the SUHI intensity is analyzed using satellite data for Budapest, the capital city of Hungary, in the Eastern/Central Europe (Fig. 1). The most important objective is to evaluate the relationship between SUHI intensity and the LCZ map of Budapest. The relationship is studied on annual, seasonal, monthly and daily scales. We analyze the SUHI intensity differences between the different LCZ classes, compare selected grid cells from the same LCZ class, and evaluate a case study for the evolution of the spatial structure of SUHI intensity.

2. DATA AND METHODOLOGY

2.1 *Satellite data*

It is preferable to use satellite data in studying the entire agglomeration area of Budapest due to the substantial spatial extension of the target area. For this purpose, remotely sensed data from satellites Terra and Aqua are used. These satellites were launched in December 1999 (Terra) and May 2002 (Aqua) as the part of the American National Aeronautics and Space Administration's (NASA) Earth Observing System (EOS).

Fig. 1: Geographical location of the target area: Budapest, Hungary located in Eastern/Central Europe.

They are on 705 km height polar orbits around the Earth with an inclination of 98°, and their orbital periods are approximately 100 minutes. Both satellites are sun-synchronous, Terra crosses the Equator on a descending orbit at 10:30 a.m., and Aqua crosses it on an ascending orbit at 1:30 p.m. Thus, for the Budapest agglomeration area, Terra can provide two images per day (at around 09-10 UTC and 20-21 UTC), as well, as Aqua (at around 02-03 UTC and 12-13 UTC). Five instruments are working on satellite Terra (NASA, 1999), and six in satellite Aqua (NASA, 2002).

Sensor MODIS (Moderate Resolution Imaging Spectroradiometer) can be found on both satellites Terra and Aqua. It measures 36 electromagnetic spectral bands, from visible to infrared (405-14385 nm). In our research, we used the following MODIS products: Land Surface Temperature (LST), and Land Cover (Strahler et al., 1999). LST is determined by using seven infrared channels (channel 20, 22, 23, 29, 31, 32, 33) with 1 km horizontal resolution derived by the method of Wan and Snyder (1999). The LST fields can be downloaded from the LP DAAC (Land Processes Distributed Active Archive Center) from 2001 till present. This way the SUHI intensity can be calculated for cloudless pixels using the average rural LST.

* *Corresponding author address*: Rita Pongrácz, Dept. of Meteorology, Eötvös Loránd University, Pázmány st. 1/a. Budapest, H-1117; Hungary; e-mail: prita@nimbus.elte.hu

2.2 *LCZ data*

The city structure is an important factor in the urban climate research. Stewart and Oke (2012) defined the LCZ system. Seven parameters represent the geometry and surface cover properties (i.e. the sky view factor, aspect ratio, building surface fraction, impervious surface fraction, pervious surface fraction, height of roughness elements, terrain roughness class) and three parameters are used for thermal, radiative, and metabolic properties (i.e. surface admittance, surface albedo, anthropogenic heat output). Seventeen LCZ classes were determined, ten built types, which depend on the height and density of the buildings, and seven surface cover types. In addition, four more variable land cover properties can be used to refine the LCZ classes (Table 1).

Table1: The LCZ classes (Stewart and Oke, 2012)

Built types	Land cover types	Variable land cover properties
LCZ 1 compact high-rise	**LCZ A** dense trees	**b** bare trees
LCZ 2 compact midrise	**LCZ B** scattered trees	**s** snow cover
LCZ 3 compact low-rise	**LCZ C** bush, scrub	**d** dry ground
LCZ 4 open high-rise	**LCZ D** low plants	**w** wet ground
LCZ 5 open midrise	**LCZ E** bare rock or paved	
LCZ 6 open low-rise	**LCZ F** bare soil or sand	
LCZ 7 lightweight low-rise	**LCZ G** water	
LCZ 8 large low-rise		
LCZ 9 sparsely built		
LCZ 10 heavy industry		

WUDAPT (World Urban Database and Access Portal Tool) is an international initiative, to collect data on the structure and functioning of cities. Bechtel et al. (2015) created a method, to prepare easily the LCZ maps of the cities. The detailed description of this method and the maps already created by the method are summarized on the WUDAPT's website (http://www.wudapt.org/). Gál et al. (2015) already prepared the LCZ maps of two Hungarian cities, the capital (Budapest) and the third most populated city (Szeged). We use the LCZ map of Budapest in this study. Because of the regional characteristics not all the 17 LCZ classes can be found in Budapest, e.g. LCZ 1 (Compact high-rise buildings) does not appear in the LCZ map of the city. The seven LCZ classes being present in Budapest are as follows:

- LCZ 2: Compact midrise
- LCZ 5: Open midrise
- LCZ 6: Open low-rise
- LCZ 8: Large low-rise
- LCZ A: Dense trees
- LCZ D: Low plants
- LCZ G: Water

2.3 *Methodology*

In this study we analyzed the relationship between the LCZ map and the SUHI intensity for Budapest, from the data of sensor MODIS between January 2001 and October 2016. We used a 70 × 70 km^2 domain of the MODIS grid cells, which include Budapest and its agglomeration, and transformed the LCZ map of Budapest (http://geopedia.world/#T4_L107_x2130299.978307 8623_y6020180.347740481_s11_b17) to this domain (Fig. 2).

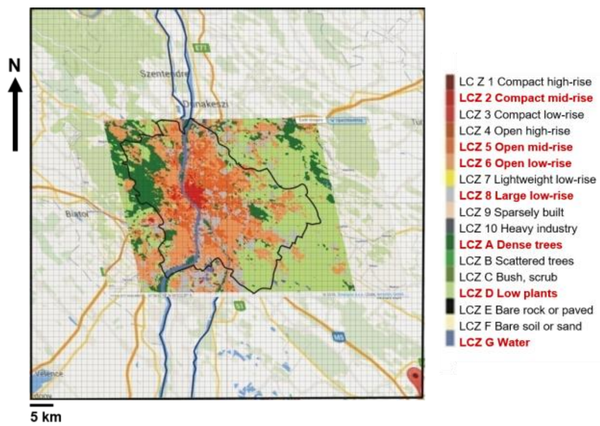

Fig. 2: The local climate zone map of Budapest transformed to the MODIS grid (70 × 70 km^2 domain). LCZ types appearing in Budapest and its close vicinity are highlighted with red.

The mains steps of the method are the following:

- to determine the LCZ class for each MODIS grid cell,
- to determine cloud coverage criteria.

The first step determines the characteristical LCZ class of each MODIS grid cell (covering 1 km^2) within the administrative boundaries of Budapest:

LCZ Class criterion 1 (LC1):
the dominant LCZ is considered in the grid cell, independently from the extent of the actual coverage of the different LCZ classes present within the grid cell;

LCZ Class criterion 2 (LC2):
the LCZ, which covers at least 50% of the grid cell;

LCZ Class criterion 3 (LC3):
the LCZ, which covers at least 75% of the grid cell.

Fig. 3 shows the number of grid cells belonging to the given LCZ class for LC1, LC2, LC3 criteria. All the grid cells can be classified according to LC1, and as the criterion becomes stricter, the total number of classified grid cells decrease, thus for example LCZ G cannot be found when using LC3. The maximum number of grid cells belong to LCZ 6 (open low-rise) when using LC1 and LC2, and LCZ D (low plants) in LC3. The minimum number of grid cells can occur in LCZ 2 (compact midrise) in the city centre.

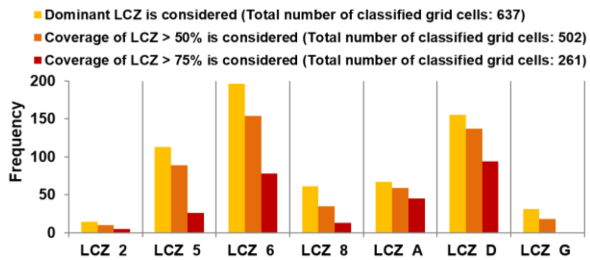

Fig. 3: The distribution of MODIS grid cells according to the LCZ types in Budapest based on the three criteria

The second step determines the cloud cover of each grid cell. The satellite sensors do not measure the land surface temperature in cloudy weather. Three cloud cover criteria are created in this analysis, depending on the extent of cloud cover in the total 70 × 70 km^2 target domain:

Cloud Cover criterion A (CCA):
less than 25% of the grid cell is covered with cloud

Cloud Cover criterion B (CCB):
less than 10% of the grid cell is covered with cloud

Cloud Cover criterion C (CCC):
0% of the grid cell is covered with cloud
(i.e. cloudless days)

3. RESULTS

3.1 *Average annual SUHI intensity distribution*

To analyze the annual distribution of SUHI intensity we used the LC2 and CCA criteria. Terra and Aqua satellites both have two passes over the target area. Fig. 4 summarizes these distributions in each LCZ classes. The evening and dawn LST is determined by long wave radiation, so that is why night-time average SUHI intensities show 1-2 °C variation throughout the whole year for each LCZ class. The day-time SUHI intensity has a substantially different annual distribution because of the shortwave radiation. The highest night-time and day-time intensity can also be found in the most built-up areas of Budapest (LCZ 2). The lowest intensity values occur in low vegetation-covered parts of the city (LCZ D) at night, and the lowest day-time SUHI intensities, negative values can be found in LCZ A, the forested areas of Budapest, because these areas of the city are cooler than the rural surroundings.

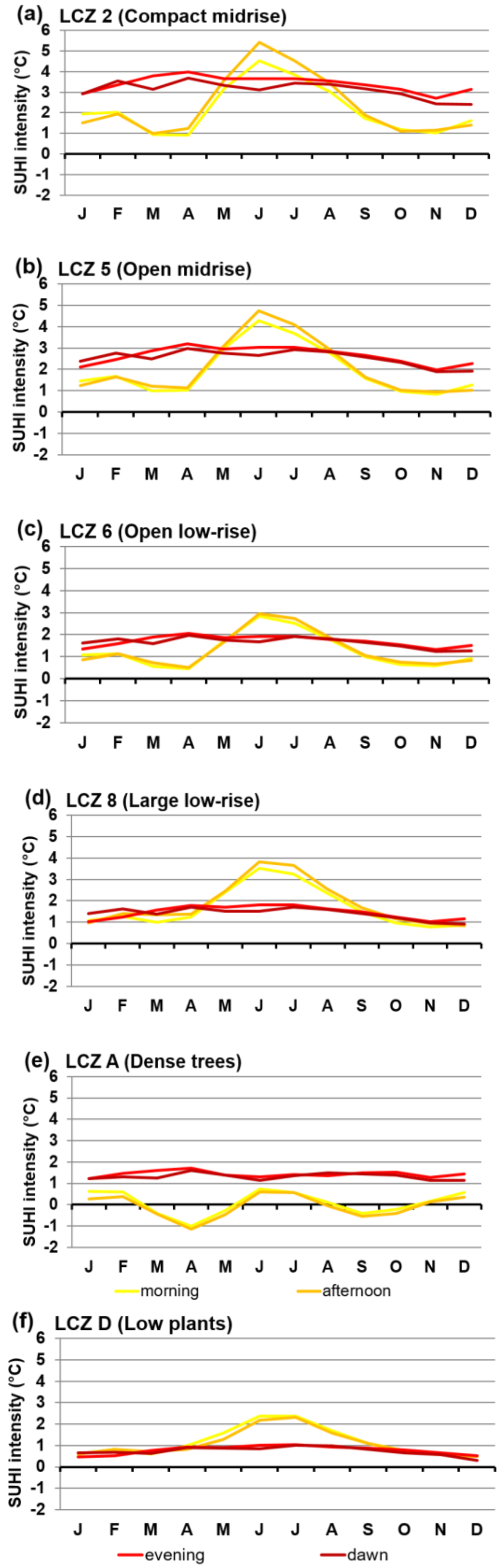

Fig. 4: Annual distribution of monthly mean SUHI intensity averaged over individual LCZ classes during the four satellite measurement times

3.2 *Comparison of grid cells classified as a given LCZ category*

In this section we used the Aqua's afternoon measurements to compare the monthly SUHI intensity time series (2003-2016) of eight selected grid cells, which are included in the same LCZ class as pairs. Table 3 and Fig. 5 summarize the selected grid cells.

The following three criteria were considered for the selection:

- the given LCZ class covers the entire grid cell;
- the grid cells from the same LCZ class should be as far from each other as possible;
- the vicinity of the selected grid cells should belong to the same LCZ class as the selected ones as much as possible.

Table 2. The LCZ type, name and location (latitude, longitude) of the selected grid cells

Grid cell	LCZ type	Name (location)
1	LCZ 2:	City Center, North (47.5°N, 19.2°E)
2	Compact mid-rise	City Center, South (47.5°N, 19.2°E)
3	LCZ 5:	Újpest (47.6°N, 19.2°E
4	Open mid-rise	Csepel (47.5°N, 19.2°E
5	LCZ 6:	Kispest (47.5°N, 19.2°E)
6	Open low-rise	Budatétény (47.4°N, 19.1°E)
7		Csillebérc (47.5°N, 19.1°E)
8	LCZ A: Dense trees	Budapesti Kamaraerdő (47.4°N, 19.1°E)

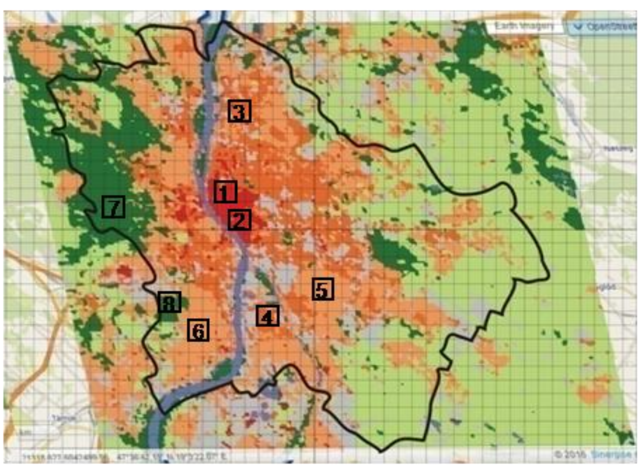

Fig. 5. The location of the grid cells selected for the comparison

To calculate the relationship between the time series we used the linear correlation coefficient (*r*) and the root-mean-square error (RMSE) with formula (1), where x_{1i} and x_{2i} are the individual values of the corresponding grid cells' time series, and n is the length of the entire time series. Due to this definition and the definition of *r*, smaller RMSE and greater *r* value indicate a greater similarity between the two compared time series.

$$RMSE = \sqrt{\frac{\sum_{i=1}^{n}(x_{1i}-x_{2i})^2}{n}} \tag{1}$$

Table 3 summarizes the RMSE and *r* values for the four compared LCZ classes, and Fig. 6 shows the time series. The smallest RMSE and the greatest correlation can be found in LCZ 2, the city center, where the two selected grid cells are close to each other. Larger differences can be observed in the time series of LCZ 5 and LCZ 6, the RMSE values are greater, and the correlations are smaller than in LCZ 2, due to the different surroundings of the grid cells. The smallest similarity is in LCZ A (Dense trees). The SUHI intensities are mostly negative in these grid cells, due to the geographical location of the grid cells. The Budapesti Kamaraerdő (8) is included in a smaller forest area, and it has a lower height above sea level (100-200 m) than Csillebérc (9) (400-500 m).

Table 3. The RMSE values and the correlation of the selected grid cells in each LCZ class

LCZ class	RMSE	*r*
LCZ 2	0.052	0.94
LCZ 5	0.165	0.81
LCZ 6	0.135	0.79
LCZ A	0.208	0.53

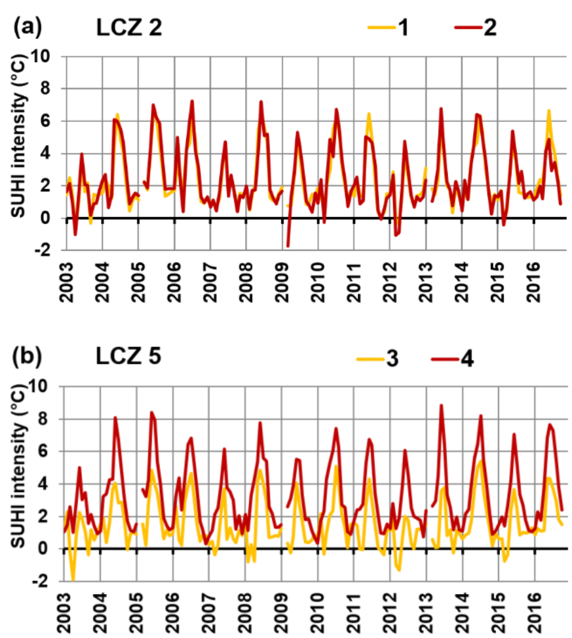

Fig. 6: Comparison of the monthly SUHI intensity time series in the selected grids cells of LCZ 2 (a) and LCZ 5 (b) based on the Aqua afternoon measurements from January 2003 to October 2016.

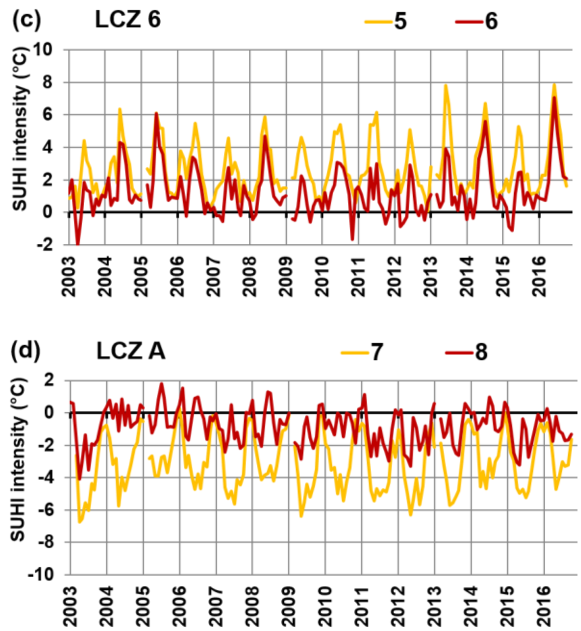

Fig. 6: Comparison of the monthly SUHI intensity time series in the selected grids cells in LCZ 6 (c) and LCZ A (d) based on the Aqua afternoon measurements from January 2003 to October 2016.

3.3 *Case study – spatial structure of SUHI intensity*

Finally, we investigated the evolution of the SUHI intensity spatial structure for a continuous cloudless period over the entire 70 × 70 km^2 domain. Most of the cloudless days occur in summer (August), therefore the studied period is selected in 26-29 August 2016. The day-time measurements of Terra and Aqua are in cloudless weather in these four days, because this period formed a heat wave event. Fig. 7 summarizes the synoptic conditions of Europe in this period. A multi-center cyclone system can be observed in western and northern Europe, and an anticyclone dominated the weather in southern and central Europe. The air temperature was 30-35 °C in Hungary (Fig. 8).

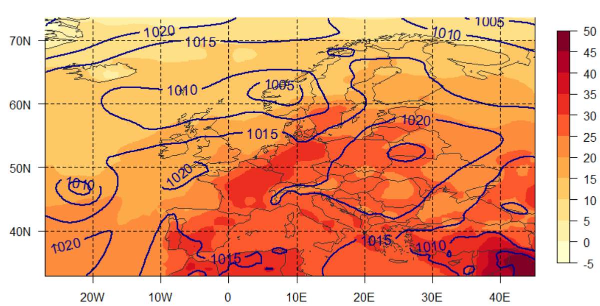

Fig. 7: Temperature (°C) and mean sea level pressure (hPa) in Europe, 12 UTC 26.08.2016. based on the ERA Interim data

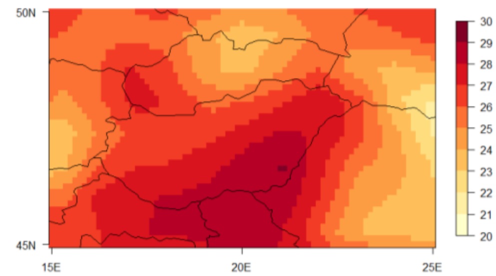

Fig. 8: Temperature (°C) in Hungary, 12 UTC 26.08.2016. based on the ERA Interim data

Fig. 9 shows the evolution of SUHI intensity spatial structure in the 70 × 70 km^2 domain. The highest SUHI intensities (7-8 °C) include the city center. Negative SUHI intensities occur in two main regions within the city: (i) the Danube, which flows through the city and the reason of the negative values is the different warming of water and land surface; (ii) the Buda Hills due to the forested coverage, and the height above sea level.

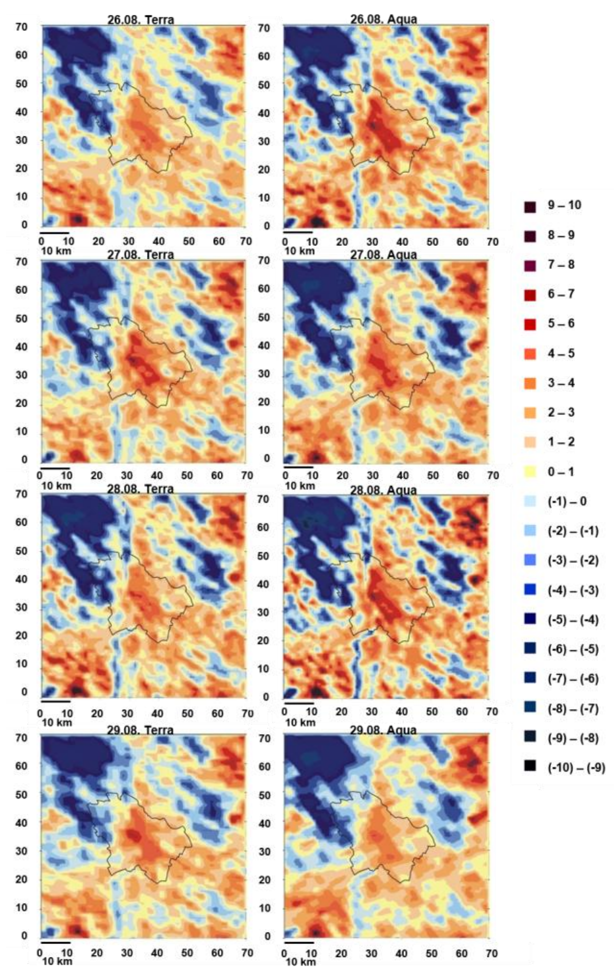

Fig. 9: Evolution of the SUHI intensity spatial structure based on Terra's morning (left) and Aqua's afternoon (right) measurements, 26-29 August 2016.

CONCLUSIONS

In this study we analyzed the SUHI intensity of the capital city of Hungary on the LCZ classes, using the surface temperature measurements of MODIS sensor in 2001-2016 and 2013-2016. We investigated SUHI intensity distribution on annual, seasonal, monthly and daily scales. Three LCZ cover criteria and three cloud cover criteria were created and used for the analysis of the SUHI intensity distributions, the comparison of some selected grid cells from the same LCZ classes, and the study of the spatial structure of SUHI intensity. The main conclusions of the study are summarized as follows. (i) The highest SUHI intensities clearly occurred in LCZ 2 (compact midrise). (ii) When the built-up density decreases, then the SUHI intensities also decrease. (iii) The lowest SUHI intensities (negative values) can be found in the vegetation-covered LCZ classes.

Acknowledgements. The authors wish to thank NASA for producing the satellite surface temperature data in their present form and the Earth Observing System Data Gateway for distributing the data. Research leading to this paper has been supported by the following sources: the Ministry of National Development of the Hungarian Government via the AGRÁRKLIMA2 project (VKSZ_12-1-2013-0034), the Széchenyi 2020 programme, the European Regional Development Fund and the Hungarian Government via the AgroMo project (GINOP-2.3.2-15-2016-00028), the Hungarian Scientific Research Fund under the grant K-120605, and the Bolyai János Research Fellowship of the Hungarian Academy of Sciences.

REFERENCES

Bartholy, J., Pongrácz, R., Dezső, Zs., Dian, Cs., Fricke, C., 2016: Recentchanges on the urban local climate using satellite data and in-situ measurements. In: *96th Annual Meeting of the American Meteorological Society*. New Orleans, LA. Paper 873, 8p. Available online at https://ams.confex.com/ams/96Annual/webprogram/Paper285360.html

Bechtel, B., Alexander, P. J., Böhner, J., Ching, J., Conrad, O., Feddema, F., Mills, G., See, L., Stewart I. D., 2015. Mapping Local Climate Zones for a Worldwide Database of the Form and Function of Cities. ISPRS International Journal of Geo-Information4, 199_219. DOI: 10.3390/ijgi4010199

Brousse, O., Martilli, A., Foley, M., Mills, G., Bechtel, B., 2016. WUDAPT, an efficient land use producing data tool for mesoscale models? Integration of urban LCZ in WRF over Madrid. Urban Climate 17, 116_134. DOI: 10.1016/j.uclim.2016.04.001

Cai, M., Ren C., Xu, Y., Dai, W., Wang, X. M., 2016. Local Climate Zone Study for Sustainable Megacities Development by Using Improved WUDAPT Methodology – A Case Study in Guangzhou. Procedia Environmental Sciences 36, 82_89. DOI: 10.1016/j.proenv.2016.09.017

Dezső, Zs., Bartholy, J., Pongrácz, R., 2005: Satellite-based analysis of the urban heat island effect. *Időjárás - Quarterly Journal of the Hungarian Meteorological Service*, 109, 217-232

Gál T., Bechtel B., Unger J., 2015. Comparison of two different Local Climate Zone mapping methods. ICUC9 conference extended abstracts. Toulouse, France, 20-24.07.2015. Paper: http://www.meteo.fr/icuc9/LongAbstracts/gd2-6-1551002_a.pdf

LCZ map of Budapest, Geopedia: http://geopedia.world/#T4_L107_x2130299.9783078623_y6020180.347740481_s11_b17

NASA, 1999: Science writers' guide to Terra. NASA EOS Project Science Office, Greenbelt, MD. 28p.

NASA, 2002: Science writers' guide to Aqua. NASA EOS Project Science Office, Greenbelt, MD. 32p.

Klysik K., Fortuniak K., 1999. Temporal and spatial characteristics of the urban heat island of Lódz, Poland. Atmospheric Environment 33, 3885_3895. DOI: S1352-2310(99)00131-4

Oke, T.R., 1973: City size and the urban heat island. *Atmospheric Environment*, 7, 769-779

Pongrácz, R., Bartholy, J., Dezső, Zs., 2010: Application of remotely sensed thermal information to urban climatology of Central European cities. *Physics and Chemistry of Earth*, 35, 95-99

Pongrácz R., Bartholy J. Dezső Zs., Dian Cs., 2016. Analysis of the air temperature and relative humidity measurements in the Budapest Ferencváros District. Hungarian Geographical Bulletin, 65(2), 93_103. DOI: 10.15201/hungeobull.65.2.1

Price, J.C., 1979: Assesment of the heat island effect through the use of satellite data. *Monthly Weather Review*, 107, 1554-1557

Stewart, I. D., Oke, T.R., 2012. Local Climate Zones for urban temperature studies. Bulletin of the American Meteorological Society, 93, 1879_1900. DOI: 10.1175/BAMS-D-11-00019.1

Strahler, A., Muchoney, D., Borak, J., Friedl, M., Gopal, S., Lambin, E., Moody, A., 1999: MODIS Land Cover Product Algorihm Theoretical Basis Document, Version 5. Center for Remote Sensing, Department of Geography, Boston University, Boston, MA. 66p.

Unger, J., Bottyan, Zs., Sumeghy, Z., Gulyas, A., 2000: Urban heat island development affected by urban surface factors. *Időjárás - Quarterly Journal of the Hungarian Meteorological Service*, 104, 253-268

Wan, Z., Snyder, W., 1999: MODIS land-surface temperature algorithm theoretical basis document. Inst. for Computational Earth Systems Science, Univ. of California, Santa Barbara. 77p.

WUDAPT (World Urban Database and Access Portal Tools): http://www.wudapt.org/